EFFECT OF COLD DRAWN DEFORMATION ON MECHANICAL PROPERTIES OF LOW CARBON STEEL DUE TO CHANGES IN GRAIN SIZE

N.A. Raji and O.O. Oluwole
Department of Mechanical Engineering, University of Ibadan, Nigeria

ABSTRACT

The effect of grain size on the mechanical properties of cold-drawn low carbon steel was investigated. Low carbon steel specimen cold-drawn to 20%, 25%, 40%, and 55% as applicable for the manufacture of 4 inches, 3 inches, 2½ inches and 2 inches nail were obtained. The study was aimed at providing experimental results for the understanding of grain size effects which occur with increasing degree of cold-drawn deformation in low-carbon steel used for nail manufacture. The micrographs of the steel were obtained using optical microscopy (OM) observation for 20%, 25%, 40%, and 55% degrees of drawn deformation. From the OM micrographs the counting method as stated in the ASTM E112 standard for grain size was used to determine the grain size of the steel on the micrograph at the different degrees of deformation. The tensile strength, yield strength, Brinnel hardness, and toughness of the materials were obtained from mechanical tests. It was shown that the tensile strength, yield strength, toughness and hardness follow quite closely the Hall-Petch equation.

Keywords: Grain size, Cold-drawn nails, Yield strength, Brinnel hardness, Tensile strength,

1.0 INTRODUCTION

The properties of polycrystalline materials depend on the microstructure and the properties of single crystals. From the viewpoint of microstructure, many factors contribute to the macroscopic properties. Grain size distribution, grain boundary and misorientation distribution are important to the mechanical properties of the material (Li et. al., [1]).

When a metal is cold drawn, the microstructure presents a morphological texture where the grains are lengthened along the wire drawing axis (Zidani et. al., [2]; Schindler et. al., [3]). Various studies had established microstructure evolution of processed materials to establish the influence of the processes on the properties of the materials. Several techniques has been used to characterize the process materials. These include the X-ray diffraction (XRD) (Babout et. al., [4]; Fiala and Němeček, [5]), transmission electron microscope (TEM) (Zhang et. al., [6]; Li et. al., [7]; Cao et. al., [8]), electron backscattering pattern (EBSP) in scanning electron microscope (SEM) (Hanton and Thomson [9]) techniques have been the primary methods of characterizing materials (Satoh et. al., [10]; Guossery et. al., [11]; Huang and Humphreys, [12]). These methods have been successfully used to determine the crystal structure, phase transformation temperatures, and precipitation behavior of annealed specimen. The microscopy techniques such as the optical microscopy or electron microscope provides spatial resolution of the microstructure ideal for static characterization at discrete processing intervals The microstructure of the material includes the shape, size, grain boundary morphology, and orientation distribution of grains in the metal (Moelans et al [13]). It is well understood that the properties of a metal are strongly influenced by these microstructure features (Crespo et. al., [14]; Ferry, [15]; Li et. al., [1]; Ganapathysubramanian and Zabaras, [16]). The microstructure of the material in which grains forming the basic matrix of the material are gradually stretched in the direction of the principal deformation and at the same time the directional arrangement of the crystallographic lattice forming structural and crystallographic texture (Schindler et. al., [3]; Schindler et. al., [17]; Zidani et. al., [2]). A typical feature of such deformed structure is anisotropy of mechanical properties where an initially isotropic material responds by developing directional anisotropy when subjected to inelastic deformation (Fuller and Brannon, [18]). The effects of such cold work on the characters of polycrystalline structures have been studied extensively (Zaefferer et. al., [19]; Ganapathysubramanian and Zabaras, [16]; Prasad et. al., [20]; Dománková et. al., [21]; Huda [22]; Pawlak and Krztoń [23]; Schindler et. al., [17]; Wert et. al., [24]; Godfrey et. al., [25]; Maurice and Driver, [26]; Basson and Driver, [27]; Godfrey et. al., [28]; Hansen and Huang, [29]).

Mechanical properties of a metal are strongly influenced by its microstructure features such as the grain size and the grain/sub-grain orientation/mis-orientation. The mechanical properties are influenced by the microstructure changes which occur during processing of the material (Ganapathysubramanian and Zabaras, [16]). The materials are commonly characterized by the average grain size and by the average misorientation between individual grains (Estrin et al., [30]). The grain size is one of the most important microstructural characteristics determining the mechanical properties and therefore the service performance of polycrystalline materials (Lu et. al., [31]; Barnett et. al., [32]). The effect of the grain size was one of the most studied size effect on plasticity. The influence of the average grain size on the mechanical properties of metals is usually described by the Hall-Patch relationship (H-P), which has been experimentally proved for a wide range of grain sizes (Keller et. al., [33]). It has been established in Hall-Petch relation that the yield strength in steels could be expressed as (Margolin, [34]);

$$\sigma_y = \sigma_0 + kd^{-1/2}$$

where σ_y is the yield stress, σ_0 and k are constants and d is the average grain size diameter. The equation was based on the idea that a dislocation source, operating from the center of a grain, produced a double pile-up at opposite sides of the grain. The stress at the head of the pile-up caused slip in the adjacent grain, which slip then spread throughout the specimen.

Investigation have revealed that the microstructure features such as the grain size and grain shapes can be controlled through effective processing design for optimum mechanical properties of the material. (Ganapathysubramanian and Zabaras, [35, 36]; Lee et al., [37]). Lee et al., [37] designed die profile in order to be able to obtain uniform grain size distribution of material during hot extrusion process. Schwaiger et al. [38] in nanoindentation and tensile test experiment revealed that strength, hardness, elastic modulus and yield strength of nanocrystalline metals depends on the strain rate of deformation which is related to the grain size. The role of grain size variation with degree of cold drawing deformation cannot therefore be overemphasized.

The several methods used for determining the grain size of material microstructure includes ultrasonic velocity technique (Sarpün et al, [39]), autocorrelation grain size analysis technique (Warrick et al, [40]), stereological methods(Liu and Yu, [41]), linear intercept measurement (Han and Kim, [42]; Thorvaldsen, [43, 44]), mathematical morphology and texture analysis (Rautio and Silvèn, [45]), image analysis (Diógenes et al., [46]), direct measurement of nucleation and growth (Lee et al., [47]), SEM image analysis (Spaulding et al, [48]), laser diffraction method (Ryżak et al.,[49]), The grain counting method, intercept method and the comparison method are the three standard test methods for determining average grain size as described in the ASTM standard E211.

In the present study low-carbon steel deformed according to specification for nail manufacture and the grain size of the microstructure at different degrees of deformation was studied, focusing on the relationship of the grain size with the yield strength, tensile strength, toughness and brinnel hardness of the steel at the 20%, 25%, 40%, and 55% degrees of cold -drawn deformation and comparing the relationship with the general Hall-Petch relationship for metal deformation.. The main objective of this work was to study the grain size and the mechanical properties of low-carbon steel with the aim of understanding the material behavior subjected to cold-drawing process as applicable to nail manufacture.

2.0 MATERIALS AND METHODS

2.1 Materials

In this study, commercially available wire rod samples drawn from as-received wire of 5.5 mm diameter to nominal diameters of 4.2 mm for 4 inches nail, 4.00 mm for 3 inches nail, 3.24 mm for 2½ inches nail and 2.35 mm for the 2 inches nail were chosen as the materials for the study. The experimental work involved the use of Optical microscopy with image capturing. The strength-elongation curves for the samples were obtained from tensile test on a Monsanto® tensometer.

2.2 Methods

2.2.1 Metallography

The as-received material is the wire rod of 5.5 mm diameter and its chemical composition is listed in Table 1. The wire rod was cold–drawn to reductions of 20%, 25%, 40% and 55% in series of conical dies on the wire drawing machines as is obtainable in Nigeria Wire Industry Limited, Ikeja. The samples for evaluation of the microstructures by optical microscopy were cut from the various deformed wires, and taken through a grinding process on silicon carbide paper, 240, 320, 400, and 600 grit. The samples were then polished initially at 1μm and finally at 0.5μm using emery cloth and silicon carbide solution. The samples were etched with 2% nital and observed under the optical microscope.

2.2.2 Mechanical testing

The samples were subjected to tensile tests to obtain the strength-ductility properties of the samples at different degree of deformation. The energy absorption at the various degrees of cold-draw deformation was obtained by determining the area under the stress-strain curve of the material using the strain energy equation defining the material toughness (Murty, [50]) expressed as;

$$U = \int_0^{\varepsilon} \sigma_e \, d\varepsilon \quad (1)$$

All the tests were performed under displacement control, so as to allow a complete recording of the load-displacement plot up to final failure.

The commonly used relationship between ultimate tensile strength (S_u) in Ksi units and Brinnel hardness number (H_B) was used in computing the Hardness property of the drawn steels. The relationship is expressed as (Bae et al., [51]);

$$S_u = 500H_B$$

This is a measure of the resistance of the material to bending during hammering.

2.2.3 Grain size measurement

The planimetric procedure for the grain counting method was used to measure the mean grain size from the obtained micrographs (Figures 1(a)–(e). The principles behind this technique and the procedure for performing it are described in the ASTM standard E112. The mean grain size is based on measurements made on the micrograph of the drawn steel at 20%, 25%, 40%, and 55% degrees of drawing deformation. The use of the mean grain size for this study was appropriate because the micrographs of the cold-drawn samples show microstructures that are geometrically similar. The ASTM micro grain size, n, was thus obtained from equation (1);

$$n = 1 + \log_2 N \quad (1)$$

Where N is the total number of grains per square inch as obtained in the procedure.

3.0 RESULTS AND DISCUSSION

The micrographs of the steel samples at 0%, 20%, 25%, 40%, and 55% degrees of cold -drawn deformation are presented in figures 1(a)-(e) showing the grain count area of 3.4 sq. in. for each of the micrograph The ASTM grain size number for each of the micrograph and the corresponding average grain size are as detail in Table 2. The mechanical properties of the cold-drawn steels are also presented in Table 2. The table shows that with increasing cold-drawing, the steel grain-diameter is larger leading to softness of the material and less toughness. This indication shows an awful reality of the situation of the nails put in the market produced by cold-drawing alone to achieve geometric (length and diameter) specifications. Figure 2 shows the results on the dependence of the yield strength on the grain size diameter of the cold-drawn low carbon steel for nail manufacture. Increase in average grain size diameter is observed with increasing degree of cold drawn deformation. Also decrease in yield strength with increasing grain size was observed in accordance with the Hall–Petch relation. It is evident from Figures 3-5 that identical relations holds for the tensile strength, toughness and hardness of the material with different coefficients K_1, K_2, K_3 and K_4. The Hall-Petch coefficient K often depends on the process parameter such as the strain rate (Estrin et al., [30]). This behavior could therefore be explained by the change of mechanism of the plastic flow of the material as it is subjected to increasing cold- drawn deformation ranging from 20%-55% for nail manufacture.

CONCLUSION

The cold- drawing process produces microstructure anisotropy in the form of increasing grain size and grain elongation in the drawing direction. This phenomenon has negative consequences on the yield strength and tensile strength of low carbon steel as well as on the toughness of the material. From experimental measurement of the yield stress of the cold- drawn low carbon steel considering the grain size *d* as the material variable which depends on the degree of drawn deformation, it has been found that the Hall-Petch relationship is satisfied. It was observed that for cold drawn low carbon steel used for nail manufacture, the increasing grain size due to increasing degree of cold drawn deformation causes reduction in the yield strength and tensile strength of the steel. The Hall-Petch coefficient which is a material property however varies under tensile deformation as observed for the yield strength, UTS and toughness Hall-Petch relationship. This established that the Hall-Petch coefficient could not always be taken as constant but dependent on the material processing condition which in this case depends on the degree of cold drawn deformation. Hence grain size dependence of the strength at various degrees of cold drawn deformation manifested in the values of the Hall–Petch coefficients. The effect can be explained by the resistance of the boundaries to plastic flow.

REFERENCES

[1] D.S., Li H., Garmestani, S., Ahzi. Processing path optimization to achieve desired texture in polycrystalline materials Acta Materialia 55: pp. 647-654 (2007)

[2] M., Zidani, M., Messaondi, C., Derfont, T., Bandin, P., Solas, M.H., Mathon Microstructure and textures evolution during annealing of a steel drawn wires. Roznov pod Radhostem, Czech Republic EU.5: pp. 18-21 (2010).

[3] I, Schindler, M. Janosec, E., Mistecky, M., R $\bar{C}_i$ $\bar{z}$ ka, L. ůž ek. Influence of cold rolling and annealing on mechanical properties of steel QStE 420. Journal of achievement in materials and Manufacturing Engineering. vol. 18(1-2): pp. 231-234. (2006)

[4] I. Babout., E. Maire., J.Y. Buffière., R. Fougères, . Characterization by X-ray computed tomography of decohesion, porosity, growth and coalescence in model metal matrix composites. Acta Materialia 49: pp. 2055-2063.(2001)

[5] J. Fiala., S. Némeček, X-ray diffraction imaging as a tool of meso structure analysis. International centre for diffraction data. Advances in X-ray analysis vol. 44: pp. 24-31 (2001).

[6] L. Zhang, T. Ohmura, K. Seikido , K. Nakajima, T. Hara., K. Tsuzaki., Direct observation of plastic deformation in iron-3% silicon single crystal by in-situ nanoindentation in transmission electron microscopy. Scripta Materialia. 4: pp.919-922 (2011)..

[7] B.Q. Li, B. Li., Y.B. Wang, M.L. Sui, E. Ma.,. Twinning Mechanism via Synchronized activation of partial dislocation in face-centred cubic materials. Scripta Materialia 64: pp. 852-855. (2011)

[8] G.H Cao., A. M Russell., K. A Gschneidner.,. Transmission electron microscopy study of the microstructure of a YCu ductile intermetallic compound, the influence of the start metal purity. Scripta Materialia 64:821-823. (2011)

[9] J. J. S Hanton., R. C.Thomson. Characterization of isothermally aged Grade 91(9Cr-1Mo-Nb-V) steel by electron backscatter diffraction. Materials Science and Enginnering A460-46: pp. 261-267. (2007).

[10] G., Satoh A., Birnibaum Y.L., Yao. Effect of annealing parameters on the shape memory properties of NiTi thin films ICALEO 2008 Congress proceedings, pp. 100-167. (2008)

[11] By V Gousserу., Y.Bienvenu, S Forest., A. F Gourgnes., C Colin., J. –D., Bartout. Grain size effects on the mechanical behavior of open-cell nikel foams. Advance Engineering Materials. vol.6(6): pp. 1-9. (2004).

[12] Y. Huang, F. J., Humphreys. Subgrain growth and low angle boundary mobility in aluminum crystals of orientation {110}<001>. Acta. Materialia 48: pp. 2017-2030. (2000)

[13] N., Moelans B., Blanpan, P.,Wollants. An introduction to phase-field modeling of microstructure evolution. Computer coupling phase diagrams and thermochemistry. 32: pp. 268-294. (2008)

[14] D., Crespo, T., Pradell, N., Clavaguera, M.T., Clavaguera-Mora. Kinetic theory of microstructural evolution in nucleation and growth processes Materials Science and Engineering A238: pp. 160- 165 (1997)

[15] M., Ferry Influence of fine particle of grain coarsening within an orientation gradient. Acta. Materialia. 53: pp. 773-783. (2005).

[16] S., Ganapathysubramanian, N., Zabaras Deformation process design for control of microstructure in the presence of dynamic recrystallization and grain growth mechanism. Int. Journal of solid and structures. vol. 41: pp. 2011-2037 (2004).

[17] J., Schindler, M., Janošec, E., Mistecky, M., Růžička, L. A.,Čížek Dobrzdviski, S., Rusz, P., Svenanek. Effect of cold rolling and annealing on mechanical properties of HSLA steel. Achives of materials Science and Engineering. vol. 36(1): pp. 41-47 (2009).

[18] T., Fuller, R.M., Brannon.. On the thermodynamic requirement of elastic stiffness anisotropy in isotropic materials. International journal of engineering science 49: pp. 311-321. (2011)

[19] S, Zaefferer, J-C, Kuo, Z., Zhao, M,Winning, D., Raabe. On the influence of the grain boundary misorientation on the plastic deformation of aluminum bicrystals. Acta Materialia. Vol. 51: pp. 4719-4735. (2003).

[20] G.V.S.S., Prasad, M., Goerdeler, G., Gottstein. Work hardening model based on multiple dislocation densities. Material Science and Engineering A 400-401: pp. 231-233. (2005).

[21] M., Domoinkova, M., Peter, M., Romanm The effect of Cold work on the sensitization of austenitic stainless steels. MTAEC 9. vol. 41(3): pp. 131-134. (2007).

[22] Z., Huda Effect of cold working and recrystallization on the mecristructure and hardness of commercial-purity aluminum. European journal of scientific research. vol. 26(4): pp. 549-557 (2009).

[23] S.J., Pawlak. H.J., Krzton, Cold Worked high alloy ultra-high strength steels with aged matensite structure. Journal of achievement in materials and engineering. vol. 36(1): pp. 18-24. (2009).

[24] J.A., Wert, Q., Liu, N., Hansen. Dislocation boundary formation in cold-rolled cube-orientation Al single crystal. Acta Materialia 45(6): pp. 2565-2576. (1997).

[25] A. Godfrey., D. J Jensen., N.Hansen, Recrystallization of channel die deformed single crystals of typical rolling orientation. Acta Materialia 49: pp. 2429-2440. (2001).

[26] C., Maurice, J.H., Driver.. Hot rolling texture of F.C.C. metals-part 1. Experimental results on Al sample and polycrystals. Acta Materialia 45(11): pp. 4627-4638. (1997)

[27] F., Bossom, J.H., Driver. Deformation banding mechanisms during plain strain compression of cube oriented F.C.C. crystals. Acta Materialia 48: pp. 2101-2115. (2000).

[28] A., Godfrey, D.J., Jensen N., Hansen Slip pattern microstructure and local crystallography in an aluminium single crystal of brass orientation {110}<112>. Acta Materialia 46(3): pp. 823-833. (1998).

[29] N., Hansen, X., Huang Microstructure and flow stress of polycrystals and single crystals. Acta Materialia 46(5): pp. 1827-1836. (1998).

[30] Y., Estrin, N.V., Isaev, S.V Lubenets, S.V.Malykhin, A.T Pugachov., V.V Pustovalov., E.N Reshetnyak., V.S Fomenko., L.S Fomenko., S.E Shumilin., M.Janecek, R.J. Hellmig. Effect of microstructure on plastic deformation of Cu at low homologous temperatures. Acta Materialia 54: pp. 5581–5590 (2006)

[31] L., Lu, A. K Dahle., D. H St.John.,. Heterogonous nucleation of Mg-Al alloys. Scripta. Materialia 54: pp. 2197-2201. (2006)

[32] M. R.Barnett, Z. Keshavarz, A. G., Beer, D.Alwell, Influence of grain size on the comprehensive deformation of wrought Mg-3Al-1Zn. Acta. Materialia. 52: pp. 5093-5103. (2004).

[33] C., Keller E., Hug, X. Feaugas.. Microstructural size effects on mechanical properties of high purity nickel. International Journal of Plasticity 27: pp. 635–654 (2011)

[34] H., Margolin Polycrystalline yielding-perspective on its onset. Acta Materialia 46(17): pp. 6305-6309. (1998).

[35] S., Ganapathysubramanian, N. Zabaras, A continuum sensitivity method for finite thermo-inelastic deformations with applications to the design of hot forming processes. International Journal for Numerical Methods in Engineering 55, pp. 1391–1437. (2002).

[36] S., Ganapathysubramanian N, Zabaras, Computational design of deformation

processes for materials with ductile damage. Computer Methods in Applied Mechanics and Engineering 192, pp. 147–183. (2003).

[37] S.K., Lee, D.C., Ko, B.M., Kim, Optimal die profile design for uniform microstructure in hot extruded product. International Journal of Machine Tools and Manufacture 40, pp. 1457–1478. (2000)

[38] R., Schwaiger, B., Moser, M., Dao Chollacoop, S.Suresh Some critical experiments on the strain-rate sensitivity of nanocrystalline nickel. Acta materialia 51: pp. 5159-5172 (2003).

[39] I.H., Sarpun, V., Ozkan, S., Tuncel R Unal.. Determination of Mean Grain Size by Ultrasonic Methods of Tungsten Carbide and Boron Carbide Composites Sintered at Various Temperatures. 4th international conference on NDT October 11-14, 2007. Chania Crete-Greece. (2007)

[40] J.A., Warrick, D.M Rubin., P., Ruggiero, J.N., Harney, A.E., Draut, D., Buscombe Cobble cam: grain-size measurements of sand to boulder from digital photographs and autocorrelation analyses Earth Surf. Process. Landforms 34, 1811–1821.(2009).

[41] G. Liu and H. Yu Experimental evaluation of stereological methods for determining 3d grain size and topological distributions. Image Anal Stereol 19: pp. 91-97 (2000).

[42] J.H. Han, and D.Y Kim., Determination of three dimensional grain size distributions by linear intercept measurement. Acta materialia. 46, No. 6, pp. 2021-2028. (1998)

[43] A. Thorvaldsen. The intercept method-1. Evaluation of grain shape. Acta Materialia. 45(2): pp. 587-594. (1997a)

[44] A. Thorvaldsen The intercept method-2. Determination of spatial grain size. Acta Materialia. 45(2): pp. 595-600. (1997b)

[45] H., Rautio and O. Silvén Average Grain Size Determination using Mathematical Morphology and Texture Analysis. *MYA '98* IAPR Workshop on Machine Vision Applications, Nov. 17-19, 1998, Makuhari, Chiba, Japan (1998).

[46] A. N., Diógenes, E. A., Hoff, C. P. Fernandes,. Grain size measurement by image analysis: An application in the ceramic and in the metallic industries. Proceedings of COBEM 2005 18th International Congress of Mechanical Engineering November 6-11, 2005, Ouro Preto, MG (2005).

[47] H.J., Lee, H.N David., T. Wu, A.G., Ramirez. Grain size estimations from the direct measurement of nucleation and growth. Applied physics letters 87: pp. 1-3 (2005)

[48] N.E., Spaulding, D.A., Meese, I., Baker, P.A., Mayewski, G.S. Hamilton. Instruments and Methods A new technique for firn grain-size measurement using SEM image analysis. Journal of Glaciology, Vol. 55, No. 195, pp. 12-19. (2010).

[49] M., Ryżak, A., Bieganowski, R.T. Walczak. Application of laser diffraction method for determination of particle size distribution of grey-brown podzolic soil. Research in agriculture engineering *53*(1): pp. 34–38 (2007)

[50] K.L Murty. 'Tension Test' http://www4.ncsu.edu/~murty/MAT450/NOTES/tandhtests.pdf(considere construction and other factors-resilience, etc) (2011)

[51] C.M Bae, W.J., Nam, C.S., Lee Effect of interlamellar spacing on the delamination of pealitic steel wires.. Scripta Materialia, vol. 35, No. 5, pp. 641-646. (1996).

Table 1 Chemical composition of the as-received steel wire material (wt %)

C	*Si*	*Mn*	*P*	*Fe*
0.12	0.18	0.14	0.7	Bal.

Table 2: Grain size and Mechanical properties strength relationship

% deformation	*ASTM grain size no.*	*Ave. grain size dia. (mm)*	*Yield strength, (N/sq. mm)*	*Tensile strength, (N/sq. mm)*	*Modulus of Toughness*	*Brinnel Hardness, HB*
Control specimen	7.47	27	80	670.88	32.88	194
20	7.15	30	70	578.79	19.42	168
25	6.9	32	60	510.12	11.25	148
40	6.67	35	44.5	392.4	8.58	114
55	6.64	38	40	382.59	4.57	111

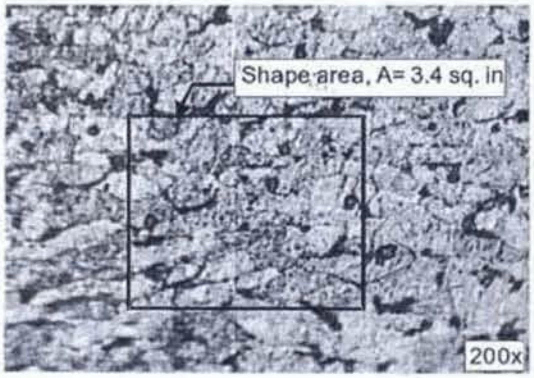

(a) Control specimen
Number grains within area = 88.7 grains/sq in
ASTM grain size no. = 7.47

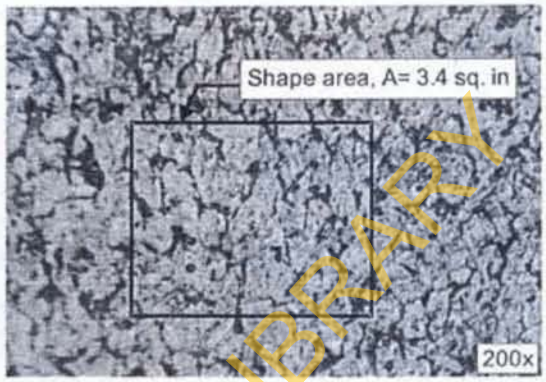

(b) 20% drawn deformation
Number grains within area =71.18 grains/sq. in
ASTM grain size no. = 7.15

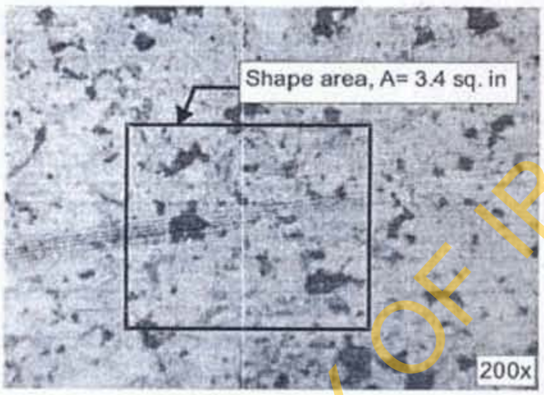

(c) 25% drawn deformation
Number grains within area =60 grains/sq. in
ASTM grain size no. = 6.90

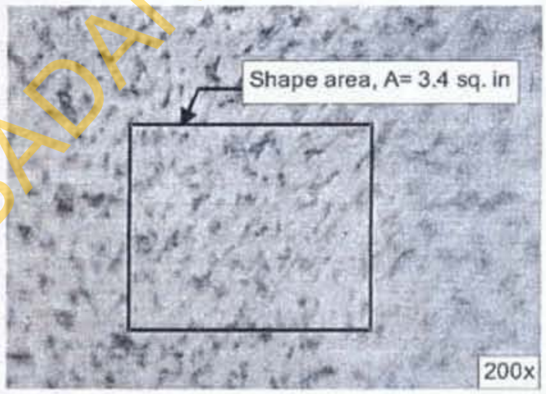

(d) 40% drawn deformation
Number grains within area =51.18 grains/sq. in
ASTM grain size no. = 6.67

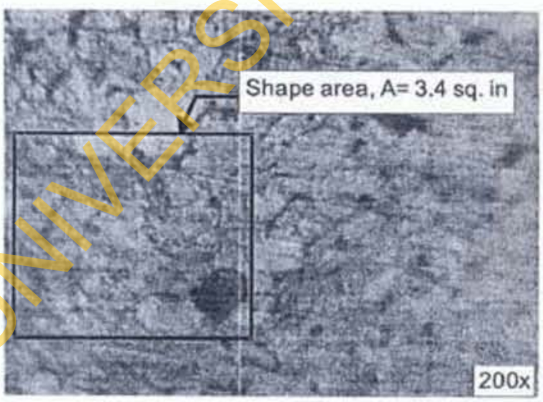

(e) 55% drawn deformation
Number grains within area =50 grains/sq. In
ASTM grain size no. = 6.64

Figure 1. Micrographs of drawn low carbon steel

Figure 2. Hall-Petch plot of yield strength for cold drawn low carbon steel

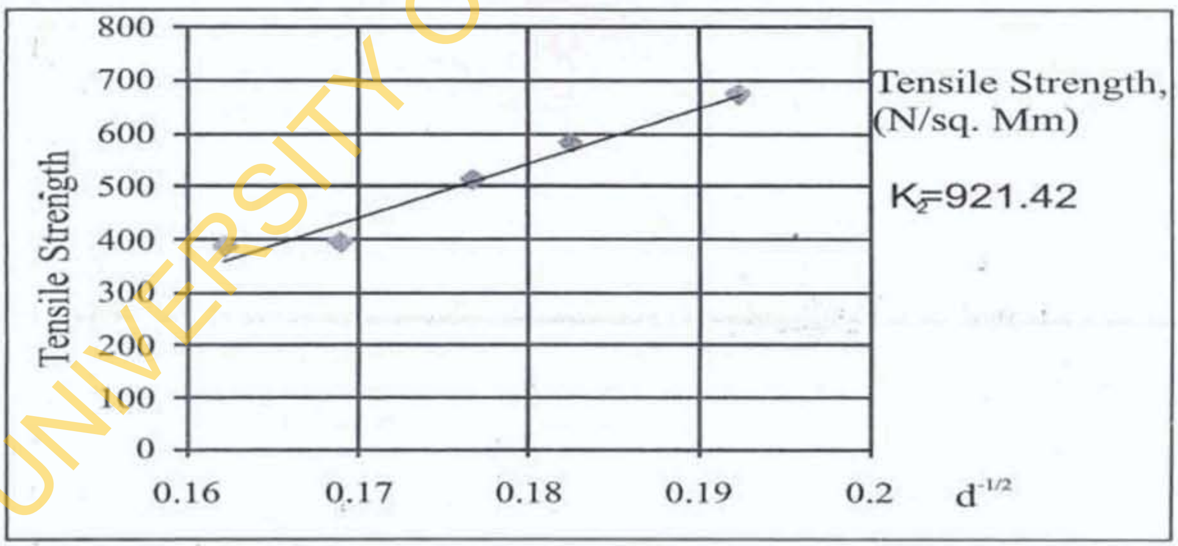

Figure 3. Hall-Petch plot of Tensile strength for cold drawn low carbon steel

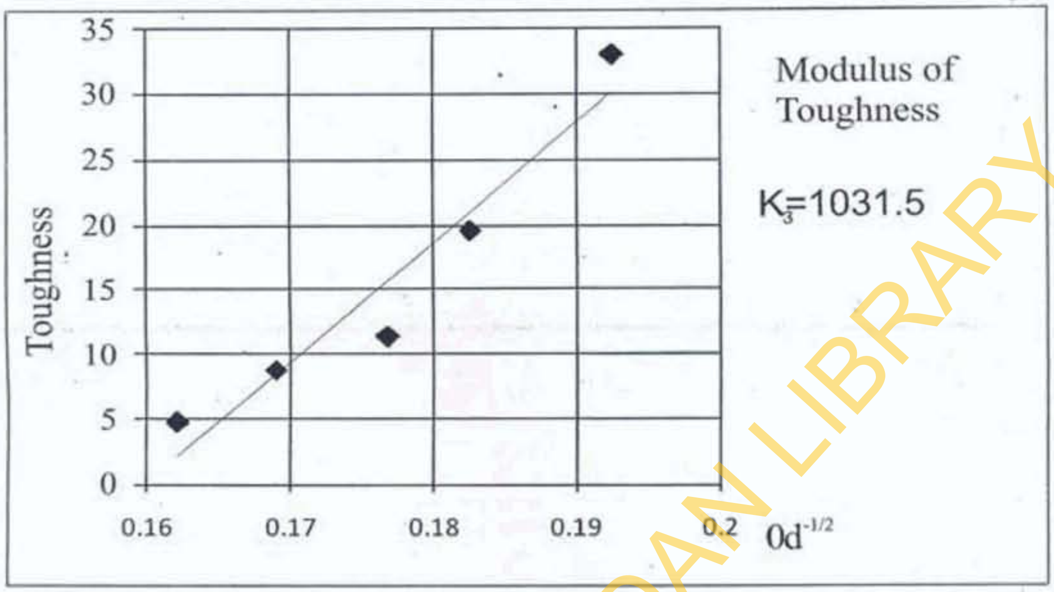

Figure 4. Hall-Petch plot of Toughness for cold drawn low carbon steel

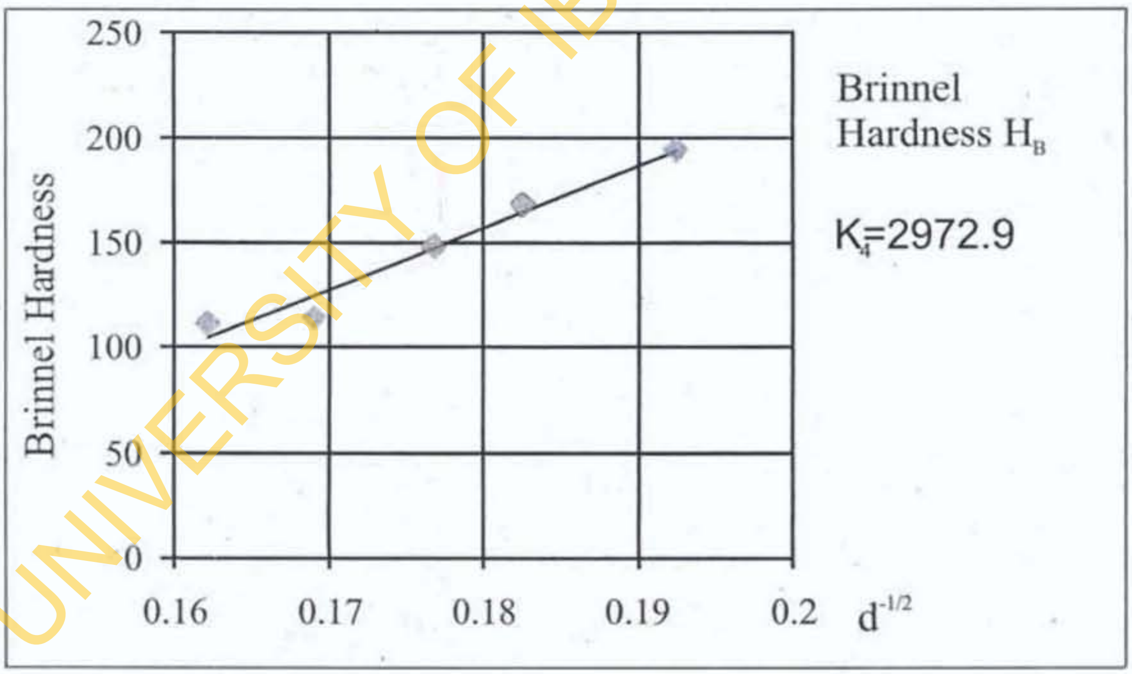

Figure 5. Hall-Petch plot of Brinnel Hardness for cold drawn low carbon steel